

# NEURAL NETWORK METHODS FOR POWER SERIES PROBLEMS OF PERRON-FROBENIUS OPERATORS

TANAKORN UDOMWORARAT\*, IGNACIO BREVIS†, MARTIN RICHTER‡, SERGIO ROJAS§, AND KRISTOFFER G. VAN DER ZEE¶

**Abstract.** Problems related to Perron-Frobenius operators (or transfer operators) have been extensively studied and applied across various fields. In this work, we propose neural network methods for approximating solutions to problems involving these operators. Specifically, we focus on computing the power series of non-expansive Perron-Frobenius operators under a given  $L^p$ -norm with a constant damping parameter in  $(0, 1)$ . We use PINNs and RVPINNs to approximate solutions in their strong and variational forms, respectively. We provide a priori error estimates for quasi-minimizers of the associated loss functions. We present some numerical results for 1D and 2D examples to show the performance of our methods.

**Key words.** neural networks, Perron-Frobenius operators, power series, physics-informed neural networks, robust variational physics-informed neural networks

**MSC codes.** 65P99, 65R20, 37N30

**1. Introduction.** Perron-Frobenius operators, also known as transfer operators, play an important role in capturing behaviors of dynamical systems. These operators have been applied to various fields of research, including engineering [35, 13], earth sciences [11], and atmospheric sciences [33, 32]. Another viewpoint to describe system behaviors is studying observables using Koopman operators, which are the adjoints of Perron-Frobenius operators. While Koopman operators track the evolution of functions on the state space, Perron-Frobenius operators describe statistical behavior through the evolution of densities [17]. These operators provide linear representations of (nonlinear) dynamical systems, which are important for estimating the long-term system behavior and prediction of future states [14].

One particularly interesting problem associated with Perron-Frobenius operators is finding the power series of these operators applied to a given initial density. The solution to this problem corresponds to the accumulated density toward the steady state, which has a direct application in finding equilibrium energy distribution [31, 27]. A classical approach for approximating solutions to problems involving such operators is Ulam’s method [34], which approximates Perron-Frobenius operators by projecting them onto a subspace spanned by characteristic functions (a space of piecewise constant functions). However, without additional effort, fixed-grid-based methods, including Ulam’s method, are known to have limitations, particularly in handling irregularities, and the convergence rate is relatively low [5].

In recent years, neural networks have been applied more and more to improve the approximate solution of various mathematical problems (see [36, 30, 26, 15, 16, 28, 7] for examples) including problems in dynamical systems (see [10, 19, 29, 23, 2, 37] for

\*School of Mathematical Sciences, University of Nottingham, United Kingdom (Tanakorn.Udomworarat@nottingham.ac.uk).

†School of Mathematical Sciences, University of Nottingham, United Kingdom (Ignacio.Brevis@nottingham.ac.uk).

‡School of Mathematical Sciences, University of Nottingham, United Kingdom (Martin.Richter@nottingham.ac.uk).

§School of Mathematics, Monash University, Australia (sergio.rojas@monash.edu)

¶School of Mathematical Sciences, University of Nottingham, United Kingdom (KG.vanderZee@nottingham.ac.uk).

examples). Among these methods, Physics-Informed Neural Networks (PINNs) [26] and various versions of Variational PINNs (VPINNs) [15, 16, 28] have gained popularity for solving equations involving operators, such as partial differential equations (PDEs). PINNs were developed to generate neural network functions to approximate solutions by minimizing a loss function based on the PDE residual. Similar methods can be found in [8, 6]. VPINNs [15] were introduced aiming to solve PDEs in variational forms, with further studies presented in [3, 4]. Robust VPINNs (RVPINNs) were developed to give a stable version of VPINNs by minimizing a loss function based on the discrete dual norm of the residual of the variational equation. Throughout this work, we use the terms PINNs and RVPINNs to refer to neural networks that encode equations describing systems by minimizing the residual of the equations in their strong and variational forms, respectively.

Neural networks offer several advantages for approximating solutions, including high expressivity [12], handling complex domains [9], and scalability to high-dimensional problems [24]. Several papers have used neural networks to learn operators in dynamical systems. For example, the authors of the seminal work [20] have proposed a deep learning framework to learn a finite-dimensional approximation of Koopman operators. However, few papers have been dedicated to studying neural networks for problems involving Perron-Frobenius operators. Applying neural networks to solve problems related to Perron-Frobenius operators, in particular power series problems, would be beneficial for approximating irregular solutions or addressing high-dimensional spaces.

In this article, we propose and analyze neural network methods for approximating solutions to power series problems for Perron-Frobenius operators with an initial density in  $L^p$ , where  $1 < p < \infty$ , considering both their strong and variational forms. Our primary focus is on Perron-Frobenius operators that are non-expansive under the  $L^p$ -norm with a constant damping parameter in  $(0, 1)$ . For consistency and simplicity, we present most results for solutions in  $L^2$  but also provide details for solutions in  $L^p$ .

The main contributions of this work are as follows. We define an abstract setting for non-expansive Perron-Frobenius operators from  $L^p$  to  $L^p$ . We establish the well-posedness of the variational formulation in  $L^2$  and  $L^p$  settings. We propose neural network methods for solving power series problems based on PINNs and RVPINNs. A key advantage of the RVPINNs approach is that it does not require the inverse map of the underlying dynamical system, as highlighted in Remark 3.1. To derive a priori error estimates for the proposed methods, we recall the concepts of neural network function manifolds and quasi-minimizers presented in [6]. The local Fortin's condition modified from [28] is required to analyze the RVPINNs method. We implement the proposed methods for approximating the power series of Perron-Frobenius operators associated with the tent map, the boundary map in a circular domain, and the standard map to show the performance of our methods. We compare our methods against a fixed-grid-based approach and the truncated sum of power series.

The article is organized as follows. In section 2, we introduce Perron-Frobenius operators, state our assumptions, present power series problems in both strong and variational forms, and provide the well-posedness of the variational problems when solutions are in  $L^2$ . We also review fixed-grid-based methods, including Ulam's method, and provide an associated error estimate. Section 3 describes neural network frameworks, including our proposed methods for approximating solutions, focusing on PINNs and RVPINNs. Section 4 is devoted to the analysis of these methods. Section 5 presents numerical examples. Section 6 is the conclusions and possible extensions. Appendix A provides the well-posedness of the variational problems when solutions

are in  $L^p$ . Appendix B shows the equivalent form of the RVPINNs loss function. Appendix C shows error estimate proofs for PINNs and RVPINNs.

**2. Abstract framework.** Let  $\Omega$  be a bounded subset of  $\mathbb{R}^d, d \geq 1$ , and  $S : \Omega \rightarrow \Omega$  be a map describing a discrete dynamical system. Given a measure space  $(\Omega, \mathcal{B}, \mu)$  where  $\mathcal{B}$  is a Borel sigma-algebra and  $\mu$  is the Lebesgue measure, the Perron-Frobenius operator associated with  $S$  is defined as the linear operator  $\mathcal{P} : L^1(\Omega) \rightarrow L^1(\Omega)$  such that

$$(2.1) \quad \int_A \mathcal{P}f d\mu = \int_{S^{-1}(A)} f d\mu, \quad \forall A \in \mathcal{B}, \forall f \in L^1(\Omega).$$

In the special case where  $\Omega = [a, b]$  is a closed interval, the Perron-Frobenius operator  $\mathcal{P}$  can be expressed explicitly (see, e.g., [18, equation 3.2.6]) as:

$$(2.2) \quad \mathcal{P}f(x) = \frac{d}{dx} \int_{S^{-1}([a, x])} f(s) ds.$$

It is well-known that the Perron-Frobenius operator  $\mathcal{P}$  is non-expansive under the  $L^1$ -norm, i.e.,  $\|\mathcal{P}f\|_{L^1} \leq \|f\|_{L^1}$  for all  $f \in L^1(\Omega)$ . For simplicity<sup>1</sup>, we consider densities  $f$  in  $L^p(\Omega)$ , where  $1 < p < \infty$ , which is a subspace of  $L^1(\Omega)$ . So, we need additional assumptions on the Perron-Frobenius operator for defining our problem in  $L^p$ -setting. In this article, we make the following assumptions:

- (A1) Density functions  $f$  are nonnegative functions in  $U := L^p(\Omega)$  with  $1 < p < \infty$ ,
- (A2)  $\mathcal{P}$  is non-expansive under the  $U$ -norm, i.e., for all  $f \in U$ ,

$$\|\mathcal{P}f\|_U \leq \|f\|_U.$$

*Remark 2.1.* The assumption (A2) holds in many dynamical systems. For instance, if  $S$  is a diffeomorphism, the Perron-Frobenius operator  $\mathcal{P}$  associated with  $S$  is given by

$$\mathcal{P}f(x) = f(S^{-1}(x)) |J_{S^{-1}}|, \quad \text{for } x \in \Omega,$$

where  $|J_{S^{-1}}|$  denotes the determinant of the Jacobian of the inverse map  $S^{-1}$  (cf. [18, Corollary 3.2.1.]). Therefore, if  $|J_{S^{-1}}| \leq 1$ ,  $\mathcal{P}$  satisfies the assumption (A2). Indeed, by applying the change of variable, we obtain

$$\begin{aligned} \|\mathcal{P}f\|_U &= \left( \int_{\Omega} (f(S^{-1}))^p |J_{S^{-1}}|^p d\mu \right)^{1/p} \\ &\leq \left( \int_{\Omega} (f(S^{-1}))^p |J_{S^{-1}}| d\mu \right)^{1/p} = \left( \int_{S^{-1}(\Omega)} f^p d\mu \right)^{1/p} = \|f\|_U. \end{aligned}$$

**2.1. Power series problem.** We are interested in approximating the solution of the following problem: Given a nonnegative function  $f_0 \in U$ , find  $u \in U$  satisfying

$$(2.3) \quad u - \alpha \mathcal{P}u = f_0,$$

where  $0 < \alpha < 1$  is a damping parameter. This is equivalent to finding the power series expressed as

$$(2.4) \quad u = f_0 + \alpha \mathcal{P}f_0 + \alpha^2 \mathcal{P}^2 f_0 + \dots$$

---

<sup>1</sup> $L^p(\Omega)$  (with  $1 < p < \infty$ ) has convenient properties for analysis such as reflexivity and strict convexity, but these properties do not hold in  $L^1(\Omega)$  [22].

*Remark 2.2.* In applications, the power series represents the equilibrium energy distribution with initial density  $f_0$ . In a more general setting, the damping parameter  $\alpha$  can be replaced by a suitable weight function  $\alpha : \Omega \rightarrow [0, \infty)$ . This would mean more realistic energy losses for individual trajectories.

**2.2. Variational problem.** The variational version of problem (2.3) is the following:

$$(2.5) \quad \text{Find } u \in U \text{ such that } b(u, v) = l(v) \quad \forall v \in V,$$

where  $V$  is the dual space of  $U$ ,  $b(\cdot, \cdot)$  and  $l(\cdot)$  are a bilinear form on  $U \times V$  and a linear functional on  $V$ , respectively, defined by

$$(2.6) \quad b(u, v) := \int_{\Omega} (u - \alpha \mathcal{P}u) v d\mu \quad \text{and} \quad l(v) := \int_{\Omega} f_0 v d\mu.$$

*Remark 2.3.* The bilinear form  $b(\cdot, \cdot)$  can be written in terms of the associated Koopman operator<sup>2</sup>  $\mathcal{K}$ , by applying the duality identity<sup>3</sup>, as follows:

$$(2.7) \quad b(u, v) := \int_{\Omega} u(v - \alpha \mathcal{K}v) d\mu.$$

This form will be used to reformulate the RVPINNs loss function in Remark 3.1.

When  $U = V = L^2(\Omega)$ , the variational problem (2.5) satisfies the conditions of the Lax-Milgram Theorem, ensuring the existence and uniqueness of the solution. The details regarding the well-posedness for  $U = L^p(\Omega)$  and  $V = L^q(\Omega)$ , where  $1 < p, q < \infty$  with  $\frac{1}{p} + \frac{1}{q} = 1$ , are provided in Appendix A.

**THEOREM 2.4** (Well-posedness of variational problem). *Given  $U = V = L^2(\Omega)$ , the variational problem (2.5) satisfies the following.*

1. *Boundedness of  $b$ :*  $|b(u, v)| \leq (1 + \alpha) \|u\|_{L^2} \|v\|_{L^2}, \quad \forall u, v \in L^2(\Omega),$
2. *Boundedness of  $l$ :*  $|l(v)| \leq \|f_0\|_{L^2} \|v\|_{L^2}, \quad \forall v \in L^2(\Omega),$
3. *Coercivity:*  $b(u, u) \geq (1 - \alpha) \|u\|_{L^2}^2, \quad \forall u \in L^2(\Omega).$

*Hence, it has a unique solution.*

*Proof.* 1. Boundedness of  $b$ : For any  $u, v \in L^2(\Omega)$ , by using the Cauchy-Schwarz inequality, the triangle inequality, and the assumption (A2), we have

$$\begin{aligned} |b(u, v)| &= \left| \int_{\Omega} (u - \alpha \mathcal{P}u) v d\mu \right| \leq \int_{\Omega} |(u - \alpha \mathcal{P}u) v| d\mu \leq \|u - \alpha \mathcal{P}u\|_{L^2} \|v\|_{L^2} \\ &\leq (\|u\|_{L^2} + \alpha \|\mathcal{P}u\|_{L^2}) \|v\|_{L^2} \leq (1 + \alpha) \|u\|_{L^2} \|v\|_{L^2}. \end{aligned}$$

2. Boundedness of  $l$ : Since  $f_0, v \in L^2(\Omega)$ , by using the Cauchy-Schwarz inequality,

$$|l(v)| = \left| \int_{\Omega} f_0 v d\mu \right| \leq \|f_0\|_{L^2} \|v\|_{L^2}.$$

<sup>2</sup>The Koopman operator associated with the map  $S$  is defined by  $\mathcal{K}v = v \circ S$ .

<sup>3</sup>Let  $1 < p, q < \infty$  with  $\frac{1}{p} + \frac{1}{q} = 1$ . If  $\mathcal{P} : L^p(\Omega) \rightarrow L^p(\Omega)$  is the Perron-Frobenius operator and  $\mathcal{K} : L^q(\Omega) \rightarrow L^q(\Omega)$  is the associated Koopman operator, then  $\int_{\Omega} (\mathcal{P}u) v d\mu = \int_{\Omega} u(\mathcal{K}v) d\mu$ .

3. Coercivity: For any  $u \in L^2(\Omega)$ , by using the Cauchy-Schwarz inequality and the assumption (A2), we have

$$\begin{aligned} b(u, u) &= \int_{\Omega} (u - \alpha \mathcal{P}u) u d\mu = \int_{\Omega} u^2 d\mu - \alpha \int_{\Omega} (\mathcal{P}u) u d\mu \\ &\geq \|u\|_{L^2}^2 - \alpha \|\mathcal{P}u\|_{L^2} \|u\|_{L^2} \geq \|u\|_{L^2}^2 - \alpha \|u\|_{L^2}^2 = (1 - \alpha) \|u\|_{L^2}^2. \quad \square \end{aligned}$$

**2.3. Fixed-grid-based method.** Let  $U = V = L^2(\Omega)$ . A classical way for solving problem (2.5) is to discretize the problem based on Galerkin projections. To do that, we first consider a finite-dimensional subspace  $V_M \subset V$  with a basis  $\{g_1, \dots, g_M\}$ . Next, we seek  $u_M \in V_M$  such that

$$(2.8) \quad b(u_M, g_m) = l(g_m) \quad \forall m \in \{1, 2, \dots, M\},$$

where  $b(\cdot, \cdot)$  and  $l(\cdot)$  are defined in (2.6). Then, as  $u_M \in V_M$ , we write  $u_M = \sum_{k=1}^M c_k g_k$  where  $c_k$  is a coefficient associated to  $g_k$ . Finally, we solve the system of equations:

$$\sum_{k=1}^M c_k \int_{\Omega} (g_k - \alpha(\mathcal{P}g_k)) g_m d\mu = \int_{\Omega} f_0 g_m d\mu, \quad m = 1, 2, \dots, M.$$

Solving this system is equivalent to solving the matrix equation  $A\mathbf{c} = \mathbf{b}$ , where the matrix entries of  $A$  are given by  $a_{mk} = \int_{\Omega} (g_k - \alpha(\mathcal{P}g_k)) g_m d\mu$  and the components of the vector  $\mathbf{b}$  are  $b_m = \int_{\Omega} f_0 g_m d\mu$ .

*Remark 2.5.* If the domain  $\Omega$  is partitioned into  $M$  subdomains  $\omega_1, \dots, \omega_M$  and  $g_m$  is chosen to be the normalized characteristic function on a subdomain  $\omega_m$ , which forms an orthonormal basis of  $V_M$ , the fixed-grid-based method is equivalent to what so-called Ulam's method [34]. The matrix equation is equivalent to  $(I_M - \alpha P_M)\mathbf{c} = \mathbf{b}$ , where  $I_M$  is the  $M \times M$  identity matrix and  $P_M$  is the matrix representation of  $\mathcal{P}$  given by  $P_M = [p_{mk}]_{M \times M}$  with

$$p_{mk} = \frac{\mu(S^{-1}(\omega_m) \cap \omega_k)}{\mu(\omega_k)}.$$

The following theorem shows an error estimate for the fixed-grid-based method.

**THEOREM 2.6.** *Let  $u_M \in V_M$  be the solution of problem (2.8) and  $u$  be the solution of problem (2.5) for  $U = V = L^2(\Omega)$ . We have*

$$\|u - u_M\|_{L^2} \leq \frac{2}{1 - \alpha} \inf_{v_m \in V_M} \|u - v_m\|_{L^2}.$$

*Proof.* For any  $v_m \in V_M$ , by using coercivity, Galerkin orthogonality, and the boundedness of  $b$ , we have

$$\begin{aligned} \|v_m - u_M\|_{L^2}^2 &\leq \frac{1}{1 - \alpha} b(v_m - u_M, v_m - u_M) \\ &= \frac{1}{1 - \alpha} [b(v_m - u, v_m - u_M) + b(u - u_M, v_m - u_M)] \\ &= \frac{1}{1 - \alpha} b(v_m - u, v_m - u_M) \\ &\leq \frac{1 + \alpha}{1 - \alpha} \|v_m - u\|_{L^2} \|v_m - u_M\|_{L^2}. \end{aligned}$$

Dividing both sides by  $\|v_m - u_M\|_{L^2}$  yields

$$\|v_m - u_M\|_{L^2} \leq \frac{1 + \alpha}{1 - \alpha} \|v_m - u\|_{L^2}.$$

Applying the triangle inequality, we have

$$\begin{aligned} \|u - u_M\|_{L^2} &\leq \|u - v_m\|_{L^2} + \|v_m - u_M\|_{L^2} \\ &\leq \|u - v_m\|_{L^2} + \frac{1 + \alpha}{1 - \alpha} \|v_m - u\|_{L^2} \\ &= \frac{2}{1 - \alpha} \|u - v_m\|_{L^2}. \end{aligned}$$

Taking the infimum over all possible  $v_m \in V_M$  yields the theorem.  $\square$

*Remark 2.7.* In the case where  $V_M$  is the space of piecewise linear finite elements defined on a mesh of size  $h$ , the error bound for a solution  $u$  in the Sobolev space  $H^2$  is of order  $O(h^2)$  (cf. [1, Theorem 1.5]).

**3. Neural network framework.** To approximate the solution of (2.3) or (2.5), we use a neural network  $u_\theta : \mathbb{R}^d \rightarrow \mathbb{R}$  where  $\theta \in \mathbb{R}^s$  represents the trainable parameters, including the networks' weights and biases. The  $L$ -layer neural network consists of an input layer,  $L-1$  hidden layers, and an output layer. Each hidden layer is a composition of an affine transformation and a nonlinear activation function. Specifically, the  $j^{th}$  hidden layer, for  $j = 1, \dots, L-1$ , is defined as

$$x^{(j)} = \phi^{(j)}(x^{(j-1)}) = \sigma(W^{(j)}x^{(j-1)} + \underline{b}^{(j)}),$$

where  $\sigma$  is an activation function,  $W^{(j)}$  and  $\underline{b}^{(j)}$  are weight matrices and bias vectors, respectively. The number of columns in  $W^{(j)}$  corresponds to the number of neurons in the  $j^{th}$  layer. The output layer follows the same structure as the hidden layers but omits the activation function, i.e.,

$$\phi^{(L)}(x^{(L-1)}) = W^{(L)}x^{(L-1)} + \underline{b}^{(L)}.$$

Thus, the  $L$ -layer neural network is expressed as

$$u_\theta(x^{(0)}) = \phi^{(L)} \circ \phi^{(L-1)} \circ \dots \circ \phi^{(1)}(x^{(0)}),$$

where  $x^{(0)}$  represents the input to the neural network. We denote  $\mathcal{M}_n$  as the set of neural network functions with a total of  $n$  neurons, based on the architecture described above:

$$\mathcal{M}_n := \{u_\theta : \mathbb{R}^d \rightarrow \mathbb{R} \mid \theta \in \mathbb{R}^s\}.$$

Assume that  $\emptyset \neq \mathcal{M}_n \subset U$ . We aim to find  $u_\theta \in \mathcal{M}_n$  such that  $u_\theta \approx u$  where  $u$  is the solution of (2.3) or (2.5). To do that, we train the neural network to minimize a loss function using some optimization methods, such as the BFGS method or Adam.

**3.1. PINNs.** To approximate the solution of problem (2.3), we follow the PINNs method by using a loss function defined in terms of the residual of the equation. The loss function<sup>4</sup> is given by:

$$(3.1) \quad \mathcal{L}_{\text{PINNs}}(u_\theta) := \|f_0 - u_\theta + \alpha \mathcal{P}u_\theta\|_U.$$

<sup>4</sup>This loss function is slightly different from the original PINNs as we do not take the square of the residual.

The approximate solution of (2.3) is obtained by solving the optimization problem:

$$(3.2) \quad \text{Find } u_{\theta^*} \in \mathcal{M}_n \text{ such that } \theta^* = \underset{\theta \in \mathbb{R}^s}{\operatorname{argmin}} \mathcal{L}_{\text{PINNs}}(u_{\theta}).$$

**3.2. RVPINNs.** For a given discrete space  $V_M \subset V$ , we consider the following Petrov-Galerkin type discretization of (2.5):

$$(3.3) \quad \text{Find } u_{\theta} \in \mathcal{M}_n \text{ such that } b(u_{\theta}, v_M) = l(v_M) \quad \forall v_M \in V_M.$$

We follow the RVPINNs method to approximate the solution of problem (3.3) by defining a loss function based on the discrete dual norm of the variational equation residual. The loss function<sup>5</sup> is given by:

$$(3.4) \quad \mathcal{L}_{\text{RVPINNs}}(u_{\theta}) := \sup_{0 \neq v_M \in V_M} \frac{l(v_M) - b(u_{\theta}, v_M)}{\|v_M\|_V}.$$

The approximate solution of (3.3) is obtained by solving the optimization problem:

$$(3.5) \quad \text{Find } u_{\theta^*} \in \mathcal{M}_n \text{ such that } \theta^* = \underset{\theta \in \mathbb{R}^s}{\operatorname{argmin}} \mathcal{L}_{\text{RVPINNs}}(u_{\theta}).$$

In practical settings, where  $U = V = L^2(\Omega)$  and  $V_M$  is a finite-dimensional subspace of  $L^2(\Omega)$  with an orthonormal basis  $\{g_m\}_{m=1}^M$ , the RVPINNs loss function can be expressed in the following equivalent form:

$$(3.6) \quad \mathcal{L}_{\text{RVPINNs}}(u_{\theta}) = \sqrt{\sum_{m=1}^M \left( \int_{\Omega} (f_0 - u_{\theta} + \alpha \mathcal{P} u_{\theta}) g_m d\mu \right)^2}.$$

The equivalence between these two forms is shown in Appendix B. It is worth noting that computing these loss functions requires numerical integration methods.

*Remark 3.1.* Using the bilinear form (2.7), we can reformulate the loss function (3.6) to eliminate the composition between the Perron-Frobenius operator  $\mathcal{P}$  and the neural network  $u_{\theta}$ . This reformulation avoids the need for the inverse map  $S^{-1}$  associated with the operator  $\mathcal{P}$ , and instead only requires the forward map  $S$  for evaluating the Koopman operator  $\mathcal{K}$  applied to the predefined test functions  $g_m$ . The resulting RVPINNs loss function is given by:

$$\mathcal{L}_{\text{RVPINNs}}(u_{\theta}) = \sqrt{\sum_{m=1}^M \left( \int_{\Omega} f_0 g_m - u_{\theta}(g_m - \alpha \mathcal{K} g_m) d\mu \right)^2}.$$

The following section presents a priori error estimates for PINNs and RVPINNs.

**4. Analysis of methods.** It is known that the manifold  $\mathcal{M}_n$  is neither a linear, a closed, nor a convex subset of  $U$  [25]. Although there is an infimum of a loss function  $\mathcal{L}$  on  $U$ , the minimizer in  $\mathcal{M}_n$  may not exist [6]. To study error analysis related to neural networks, we will use a relaxed definition of a minimizer called a quasi-minimizer (cf. [6]).

**DEFINITION 4.1.** Let  $\mathcal{L} : U \rightarrow \mathbb{R}$  be a loss function and  $\delta_n > 0$ . A function  $u_{\theta^*} \in \mathcal{M}_n \subset U$  is said to be a quasi-minimizer of  $\mathcal{L}$  if

$$(4.1) \quad \mathcal{L}(u_{\theta^*}) \leq \inf_{u_{\theta} \in \mathcal{M}_n} \mathcal{L}(u_{\theta}) + \delta_n.$$

<sup>5</sup>This loss function is slightly different from the original RVPINNs as we do not take the square of the residual.

#### 4.1. Error estimate for PINNs.

**THEOREM 4.2.** *Let  $\delta_n > 0$  and  $u_{\theta^*} \in \mathcal{M}_n$  be a quasi-minimizer of (3.1) satisfying (4.1). If  $u$  is the solution of (2.3), we have*

$$\|u - u_{\theta^*}\|_U \leq \left( \frac{1 + \alpha}{1 - \alpha} \right) \inf_{u_{\theta} \in \mathcal{M}_n} \|u - u_{\theta}\|_U + \frac{\delta_n}{1 - \alpha}.$$

*Proof.* See details of the proof in Appendix C.  $\square$

**4.2. Error estimate for RVPINNs.** To obtain a reliable error bound for the RVPINNs method, we need the following assumption.

**Local Fortin's condition**<sup>6</sup>: Let  $\delta_n > 0$  and  $u_{\theta^*} \in \mathcal{M}_n$  be a quasi-minimizer of  $\mathcal{L}_{\text{RVPINNs}}$  satisfying (4.1). There exists  $R > 0$  such that for all  $\theta \in B(\theta^*, R)$ , an operator  $\Pi_{\theta} : V \rightarrow V_M$  and  $\theta$ -independent constant  $C_{\Pi} > 0$ , satisfying:

1.  $b(u_{\theta^*} - u_{\theta}, v - \Pi_{\theta}v) = 0, \quad \forall v \in V,$
2.  $\|\Pi_{\theta}v\|_V \leq C_{\Pi}\|v\|_V, \quad \forall v \in V,$

where  $B(\theta^*, R)$  is an open ball of center  $\theta^*$  and radius  $R$ , with respect to a given norm of  $\mathbb{R}^n$ . We denote  $\mathcal{M}_n^{\theta^*, R} := \{u_{\theta} \in \mathcal{M}_n : \theta \in B(\theta^*, R)\}$ .

**THEOREM 4.3.** *Let  $\delta_n > 0$  and  $u_{\theta^*} \in \mathcal{M}_n$  be a quasi-minimizer of (3.4) satisfying (4.1). If the local Fortin's condition is satisfied, we have*

$$\|u - u_{\theta^*}\|_U \leq \left( 1 + \frac{2(1 + \alpha)C_{\Pi}}{1 - \alpha} \right) \inf_{u_{\theta} \in \mathcal{M}_n^{\theta^*, R}} \|u - u_{\theta}\|_U + \left( \frac{C_{\Pi}}{1 - \alpha} \right) \delta_n.$$

*Proof.* See details of the proof in Appendix C.  $\square$

**5. Numerical examples.** In this section, we show the performance of PINNs and RVPINNs for power series problems by applying them to various 1D and 2D dynamical systems. We focus on systems where Perron-Frobenius operators are non-expansive under the  $L^2$ -norm.

**5.1. 1D dynamical systems.** We consider the dynamical system described by the tent map, which is a simple, continuous, piecewise-linear function exhibiting chaotic behavior. The tent map  $S : [0, 1] \rightarrow [0, 1]$  is defined as:

$$S(x) = \begin{cases} 2x, & x \in [0, \frac{1}{2}), \\ 2 - 2x, & x \in [\frac{1}{2}, 1]. \end{cases}$$

By applying equation (2.2), the Perron-Frobenius operator associated with the tent map can be derived in the form of

$$(5.1) \quad \mathcal{P}f(x) = \frac{1}{2}f\left(\frac{x}{2}\right) + \frac{1}{2}f\left(1 - \frac{x}{2}\right),$$

and we can verify that it is non-expansive under the  $L^2$ -norm. Indeed,

$$\begin{aligned} \|\mathcal{P}f\|_{L^2}^2 &= \int_0^1 \left( \frac{1}{2}f\left(\frac{x}{2}\right) + \frac{1}{2}f\left(1 - \frac{x}{2}\right) \right)^2 dx \\ &\leq \frac{1}{2} \int_0^1 f^2\left(\frac{x}{2}\right) + f^2\left(1 - \frac{x}{2}\right) dx = \int_0^1 f^2(x) dx = \|f\|_{L^2}^2. \end{aligned}$$

<sup>6</sup>Item 1 of this condition has been modified from Assumption 1 in [28], as we will derive an a priori error estimate for RVPINNs in terms of the infimum over  $\mathcal{M}_n^{\theta^*, R}$ , which is a more natural form compared to the infimum over  $\text{span}(\mathcal{M}_n^{\theta^*, R})$  used in [28].



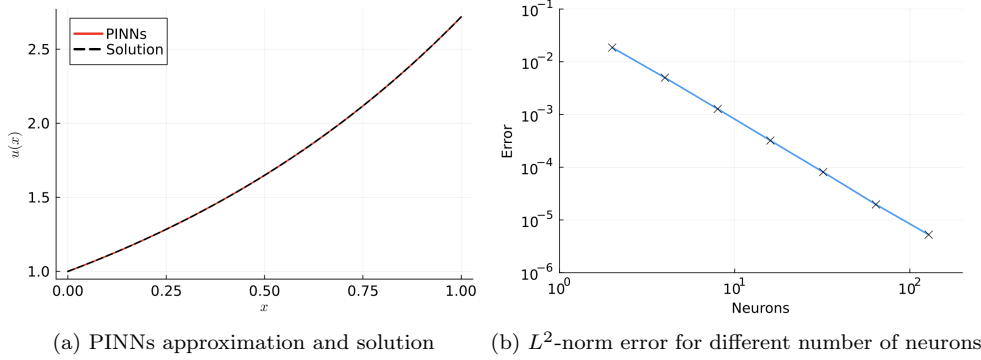


Fig. 1: PINNs approximation for  $u^{[1]}$  with  $\alpha = 0.5$ .

Because it is challenging to obtain analytical solutions of (2.3), we design our examples in reverse order: We specify a desired solution and then determine the corresponding initial density. This approach allows us to create well-defined test cases. For the Perron-Frobenius operator  $\mathcal{P}$  given in (5.1), we implement PINNs and RVPINNs to approximate two types of solutions:

1. A smooth solution  $u^{[1]}(x) = \exp(x)$ ,
2. A singular solution  $u^{[2]}(x) = 1 + x^{-1/3}$ .

To construct the initial densities  $f_0^{[i]}$  corresponding to these solutions, we substitute the desired solution  $u^{[i]}$  into (2.3) and derive the following initial densities:

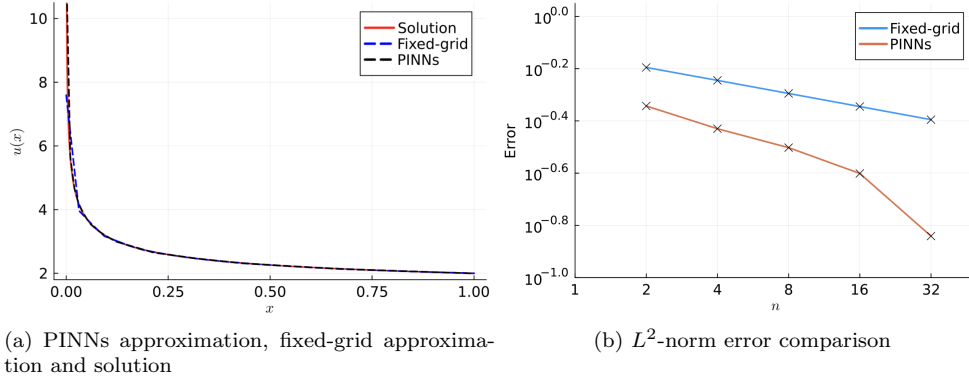
1.  $f_0^{[1]}(x) = \exp(x) - \frac{\alpha}{2} \exp\left(\frac{x}{2}\right) - \frac{\alpha}{2} \exp\left(1 - \frac{x}{2}\right)$ ,
2.  $f_0^{[2]}(x) = (1 - \alpha) + x^{-1/3} - \frac{\alpha}{2} \left(\frac{x}{2}\right)^{-1/3} - \frac{\alpha}{2} \left(1 - \frac{x}{2}\right)^{-1/3}$ .

We note that  $f_0^{[1]}$  and  $f_0^{[2]}$  are nonnegative when  $\alpha \leq 2/(1 + e)$  and  $\alpha \leq 2/(1 + \sqrt[3]{2})$ , respectively.

To show the performance of the PINNs approach, we apply it to approximate the solution  $u^{[1]}$ . In the loss function (3.1), we use the corresponding initial density  $f_0^{[1]}$ , set the damping parameter to  $\alpha = 0.5$ , and use the Perron-Frobenius operator  $\mathcal{P}$  as defined in (5.1). The neural network architecture consists of a single hidden layer with  $n$  neurons and the ReLU activation function ( $\text{ReLU}(x) = \max(x, 0)$ ), i.e.,

$$(5.2) \quad u_\theta(x) := \sum_{j=1}^n c_j \text{ReLU}(w_j x + b_j) + c_0,$$

where  $c_j, w_j, b_j \in \mathbb{R}$  are trainable parameters. The neural network is initialized to produce a piecewise-linear approximation over a uniform partition of  $[0, 1]$  into  $n$  subintervals, with the outer parameters  $c_j$  chosen to minimize the PINNs loss function. To approximate the integral in the loss function, we use a 101-point Gauss-Kronrod quadrature rule. We train the neural network using the BFGS algorithm to minimize the loss function. Figure 1 (a) shows the PINNs approximation using the neural network with  $n = 32$  neurons, which presents a good approximation to the solution. Figure 1 (b) demonstrates  $L^2$ -norm errors for trained neural networks,  $\|u - u_\theta\|_{L^2}$ , for different numbers of neurons. The slope of the plot is approximately  $-2$ , confirming that the convergence rate is  $O(n^{-2})$ , as expected for continuous piecewise-linear

Fig. 2: PINNs approximation for  $u^{[2]}$  with  $\alpha = 0.5$ .

$n$	Fixed-grid	PINNs
2 – 4	0.164	0.289
4 – 8	0.166	0.241
8 – 16	0.167	0.328
16 – 32	0.167	0.796

Table 1: Experimental order of convergence for the fixed-grid-based method with  $n$  breakpoints and PINNs with  $n$  neurons.

approximations (see Remark 2.7).

To compare PINNs with the fixed-grid-based method, we consider the singular solution  $u^{[2]}$ . In the fixed-grid-based method, the domain is partitioned into  $n$  equal-length subintervals, and hat functions defined over these intervals are used as basis functions. In the PINNs approach, we use an  $n$ -neuron neural network as defined in (5.2). The inner parameters  $w_j$  and  $b_j$  are initialized to generate breakpoints at  $r, r^2, \dots, r^{n-1}$ , and 0 with  $r = 0.662$ , while the outer parameters  $c_j$  are chosen to minimize the PINNs loss function for the given inner parameters. Under these settings, the fixed-grid-based method and PINNs produce piecewise-linear approximations with  $n$  breakpoints. Since the target function is singular, we use a finer quadrature rule with 501 points to improve integration accuracy. Figure 2 (a) shows that PINNs achieve greater accuracy than the fixed-grid-based method when both use  $n = 32$ . Furthermore, Figure 2 (b) illustrates that the  $L^2$ -norm error for PINNs is smaller than that of the fixed-grid-based method, highlighting their superior approximation capability. Table 1 reports the experimental order of convergence (EOC) corresponding to Figure 2 (b). The EOC for the fixed-grid-based method is approximately  $1/6$ , consistent with the theoretical convergence rate  $O(n^{-1/6})$  for a uniform grid, based on a Sobolev embedding argument as discussed in Example 5.8 of [21]. Additionally, as expected for a free-knot method, the EOC for PINNs shows a superior convergence rate.

The RVPINNs method provides an alternative approach for approximating solutions to power series problems. We use the same neural network structure as the PINNs examples. The domain is partitioned into eight equal-length intervals, with

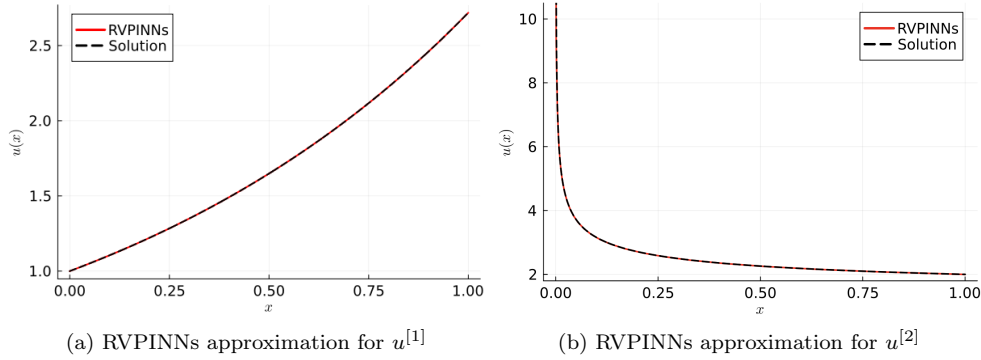


Fig. 3: RVPINNs approximation for the tent map example.

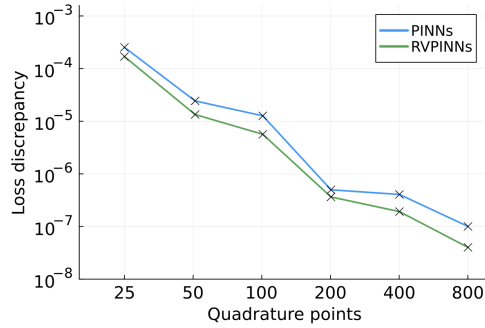


Fig. 4: The discrepancy between the loss function computed using different numbers of quadrature points and the true value of the loss function.

the test functions chosen as normalized characteristic functions over these intervals. Figures 3 (a) and 3 (b) illustrate that the trained 32-neuron neural networks, using the RVPINNs method, generate accurate approximations for both examples.

Since our implementation relies on numerical integration using the Gauss-Kronrod quadrature rule, we examine the discrepancy between the loss function computed with  $q$  quadrature points and that obtained using the adaptive Gauss-Kronrod quadrature rule, which we treat as the exact value (with an error tolerance below  $10^{-8}$ ). As shown in Figure 4, the approximation error in the loss function decreases as the number of quadrature points increases.

**5.2. 2D dynamical systems.** Now, we will show the performance of PINNs and RVPINNs in 2D examples. We consider the boundary map in a circular domain and the standard map. In a circular domain, positions of rays can be described by a coordinate  $(\varphi, \psi)$  where  $\varphi \in [0, 2\pi)$  describes the position on the boundary, given by polar angle, and  $\psi \in (-\frac{\pi}{2}, \frac{\pi}{2})$  describes a direction after a collision, given by the angle between the normal line of the circle and the reflected ray. Let  $\Omega := [0, 2\pi) \times (-\frac{\pi}{2}, \frac{\pi}{2})$ . The boundary map in a circular domain is a function  $S_1 : \Omega \rightarrow \Omega$  defined by

$$S_1(\varphi, \psi) = (\varphi + \pi - 2\psi \mod 2\pi, \psi),$$

and its inverse map is

$$S_1^{-1}(\varphi, \psi) = (\varphi - \pi + 2\psi \mod 2\pi, \psi).$$

The standard map is a mathematical model used to study chaotic behavior in dynamical systems. It is a discrete-time dynamical system that exhibits a transition from regular to chaotic motion, making it a popular example in the study of chaos theory. The standard map  $S_2$  is a mapping from  $[0, 2\pi) \times [0, 2\pi)$  to itself defined by

$$S_2(\theta, p) = (\theta + p + K \sin(\theta) \mod 2\pi, p + K \sin(\theta) \mod 2\pi),$$

and its inverse map is

$$S_2^{-1}(\theta, p) = (\theta - p \mod 2\pi, p - K \sin(\theta - p) \mod 2\pi),$$

where  $K$  is a parameter that controls the amount of chaos in the system. In this work, we use  $K = 2.4$ .

Note that the boundary map and the standard map satisfy Remark 2.1 with  $|J_{S_i^{-1}}| = 1$ , so the Perron-Frobenius operators associated with  $S_i$  are in the form  $\mathcal{P}f = f(S_i^{-1})$ .

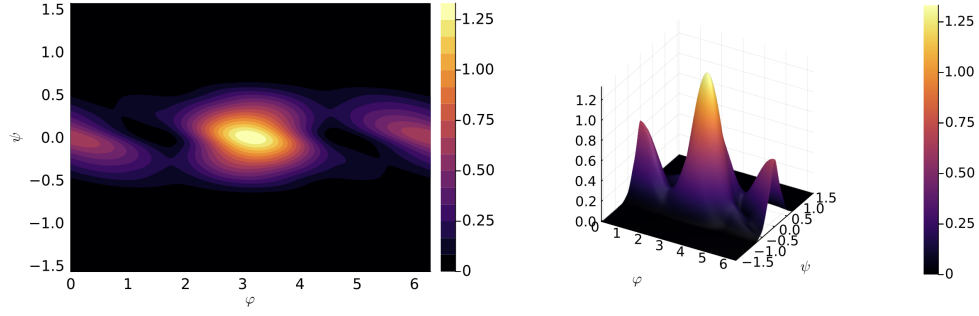
We implement PINNs and RVPINNs to approximate the solution of (2.3) and (2.5), respectively, for the Perron-Frobenius operator associated with the boundary map. We set the damping parameter  $\alpha = 0.5$ . The initial density is given by  $f_0(\varphi, \psi) = \cos^2(\varphi) \cos^2(2\psi)$  for  $\pi/2 < \varphi < 3\pi/2$  and  $-\pi/4 < \psi < \pi/4$ , and 0 elsewhere. For RVPINNs, we partition the domain into  $8 \times 8$  equal-sized cells, denoted as  $\omega_1, \dots, \omega_{64}$ , and define  $g_m$  as the normalized characteristic function on  $\omega_m$ . We use a two-layer neural network, 32 neurons, and the ReLU activation function, i.e.,

$$u_\theta(x, y) := \sum_{j=1}^{32} c_j \text{ReLU}(w_j^{(1)} x + w_j^{(2)} y + b_j) + c_0,$$

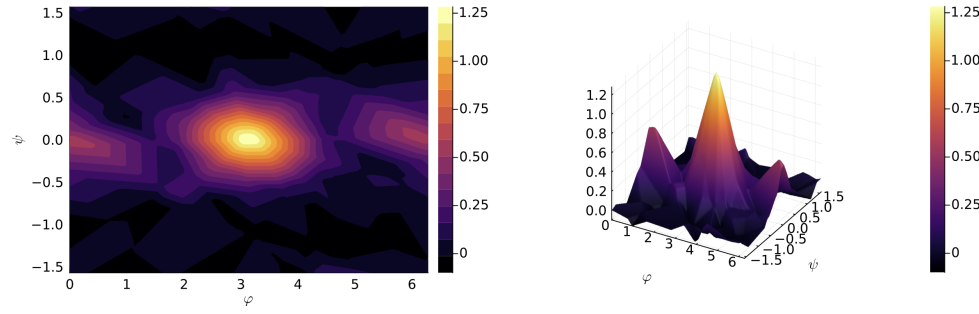
where  $c_j, w_j^{(1)}, w_j^{(2)}, b_j \in \mathbb{R}$  are trainable parameters. We approximate double integrals in PINNs and RVPINNs loss functions using a 101-point Gauss-Kronrod quadrature rule for each variable. After training the neural network using Adam optimizer, we obtain approximations that closely match the truncated sum of (2.4) with 1,000 terms, as shown in Figures 5 and 6. Despite using a relatively small neural network, it achieves a good approximation.

We also apply PINNs and RVPINNs to the standard map example, where the initial density is given by  $f_0(\theta, p) = \cos^2(2\theta) \cos^2(2p)$  for  $3\pi/4 < \theta < 5\pi/4$  and  $3\pi/4 < p < 5\pi/4$ , and 0 elsewhere. As  $\alpha$  increases, power series for the standard map example become more complex, as shown in Figure 7. To make neural networks converge to complex solutions faster, we employ a continuation technique: training the neural network to approximate solutions for small  $\alpha$ , then using the resulting model as an initialization for training with larger  $\alpha$ . We train neural networks using the same approach described above. Figure 8 shows the approximate solutions obtained with PINNs for various values of  $\alpha$ . Similar results were observed for RVPINNs, which are therefore omitted for brevity. These results demonstrate that PINNs and RVPINNs can capture the key features of solutions in dynamical systems.

**6. Conclusions.** In this article, we investigated power series problems associated with non-expansive Perron-Frobenius operators under the  $L^p$ -norm, with a focus

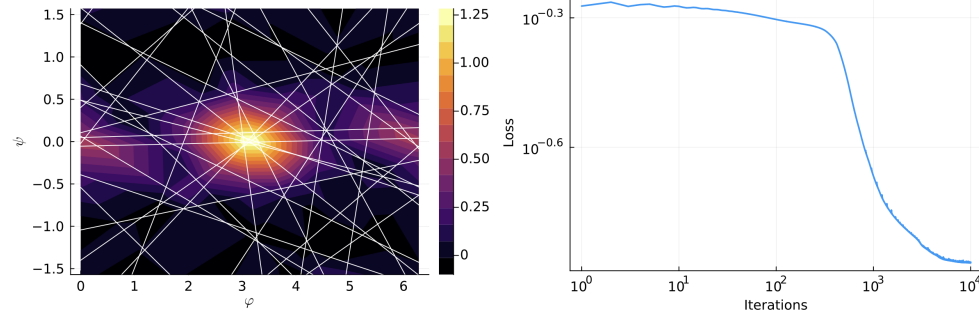


(a) 2D plot of the truncated sum with 1,000 terms (b) 3D plot of the truncated sum with 1,000 terms



(c) 2D plot of PINNs approximation

(d) 3D plot of PINNs approximation



(e) 2D plot of PINNs approximation with straight lines representing the affine transformations in the hidden layer

(f) Loss plot

Fig. 5: PINNs approximation for the boundary map example.

on the  $L^2$ -setting. We established the well-posedness of the corresponding variational formulations in  $L^2$  by showing that they satisfy the conditions of the Lax-Milgram theorem, thereby ensuring the existence and uniqueness of solutions. We proposed two neural network methods for approximating solutions of power series problems. PINNs were employed to approximate solutions in their strong form, while RVPINNs were used to approximate solutions in the corresponding variational problems. Additionally, we provided error estimates for both methods in terms of quasi-minimizers. Nu-

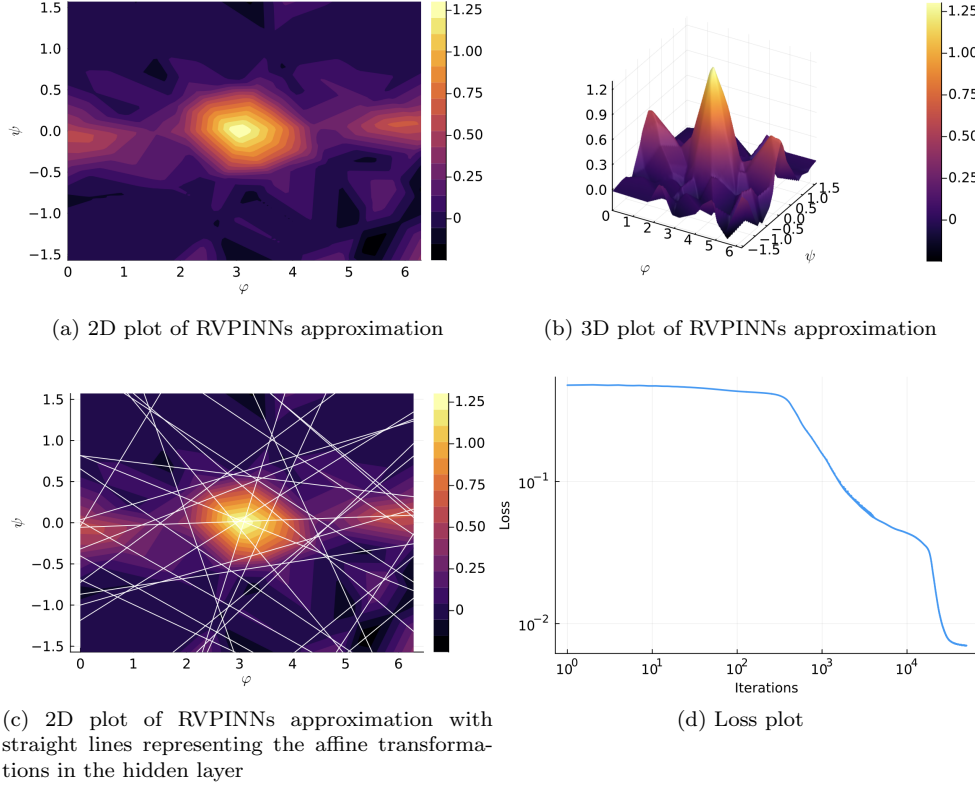


Fig. 6: RVPINNs approximation for the boundary map example.

merical experiments demonstrated that both methods are effective for solving power series problems and outperform the standard fixed-grid-based method.

Further extensions of this work include applying power series approximations to real-world applications involving complex dynamical systems. Moreover, the theoretical results in this paper, such as a priori error estimates based on the local Fortin's condition, could be applied to establish reliable error bounds for solving PDEs with neural networks.

**Acknowledgments.** T. Udomworarat was supported by the Royal Thai Government Scholarship under the Office of Educational Affairs, the Royal Thai Embassy in London. I. Brevis was supported by the Engineering and Physical Sciences Research Council (EPSRC), UK, under Grant EP/W010011/1. S. Rojas's work was supported by the Chilean grant ANID FONDECYT No. 1240643.

#### Appendix A. Well-posedness of variational problems for $L^p - L^q$ spaces.

In the following, we show that the variational problem (2.5) satisfies the assumptions of Banach-Nečas-Babůska Theorem, so the existence and uniqueness of the solution are verified.

**THEOREM A.1** (Well-posedness of variational problem). *If  $U = L^p(\Omega)$  and  $V =$*

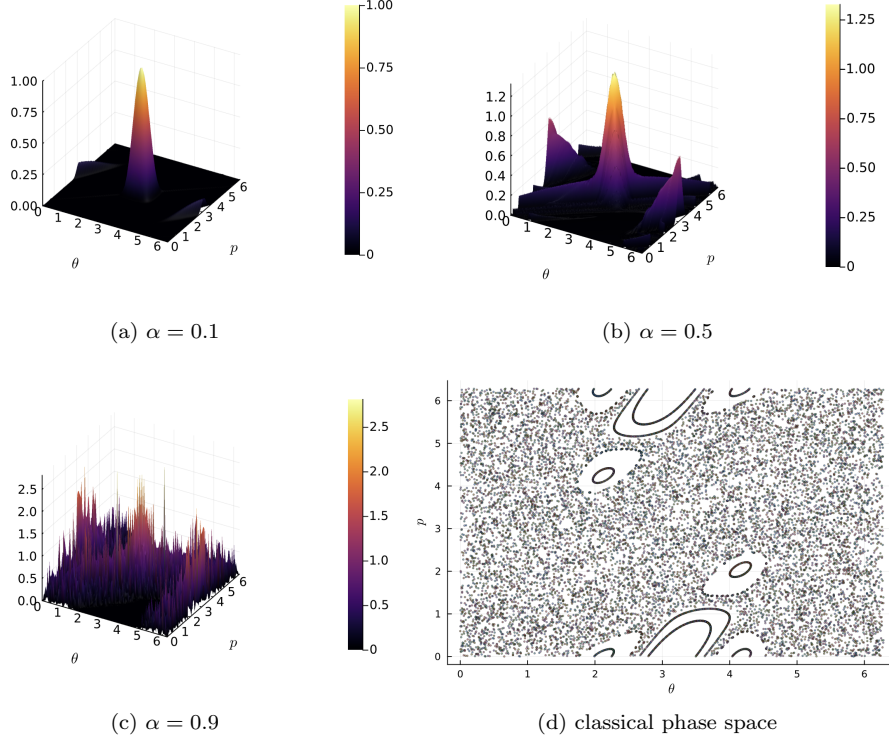


Fig. 7: (a)-(c) 3D plots of the truncated sum with 1,000 terms for the standard map example with different values of  $\alpha$ , and (d) a classical phase space showing the distribution of point trajectories in the system.

$L^q(\Omega)$ , where  $1 < p, q < \infty$  and  $\frac{1}{p} + \frac{1}{q} = 1$ . The variational problem (2.5) satisfies the following:

1. Boundedness of  $b$ :  $|b(u, v)| \leq (1 + \alpha)\|u\|_{L^p}\|v\|_{L^q}$ ,  $\forall u \in L^p(\Omega), v \in L^q(\Omega)$ ,
2. Boundedness of  $l$ :  $|l(v)| \leq \|f_0\|_{L^p}\|v\|_{L^q}$ ,  $\forall v \in L^q(\Omega)$ ,
3. Inf-sup stability:  $\sup_{0 \neq v \in L^q(\Omega)} \frac{b(u, v)}{\|v\|_{L^q}} \geq (1 - \alpha)\|u\|_{L^p}$ ,  $\forall u \in L^p(\Omega)$ ,
4. Adjoint injectivity:  $b(u, v) = 0 \quad \forall u \in L^p(\Omega) \implies v = 0$ .

Hence, the variational problem (2.5) has a unique solution.

*Proof.* 1. Boundedness of  $b$ : For  $u \in L^p(\Omega)$  and  $v \in L^q(\Omega)$ , by using Hölder's inequality, the triangle inequality, and the assumption (A2), we have

$$\begin{aligned}
 |b(u, v)| &= \left| \int_{\Omega} (u - \alpha \mathcal{P}u) v d\mu \right| \leq \int_{\Omega} |(u - \alpha \mathcal{P}u) v| d\mu \leq \|u - \alpha \mathcal{P}u\|_{L^p} \|v\|_{L^q} \\
 &\leq (\|u\|_{L^p} + \alpha \|\mathcal{P}u\|_{L^p}) \|v\|_{L^q} \leq (1 + \alpha) \|u\|_{L^p} \|v\|_{L^q}.
 \end{aligned}$$

2. Boundedness of  $l$ : Since  $f_0 \in L^p(\Omega), v \in L^q(\Omega)$ , by using Hölder's inequality,

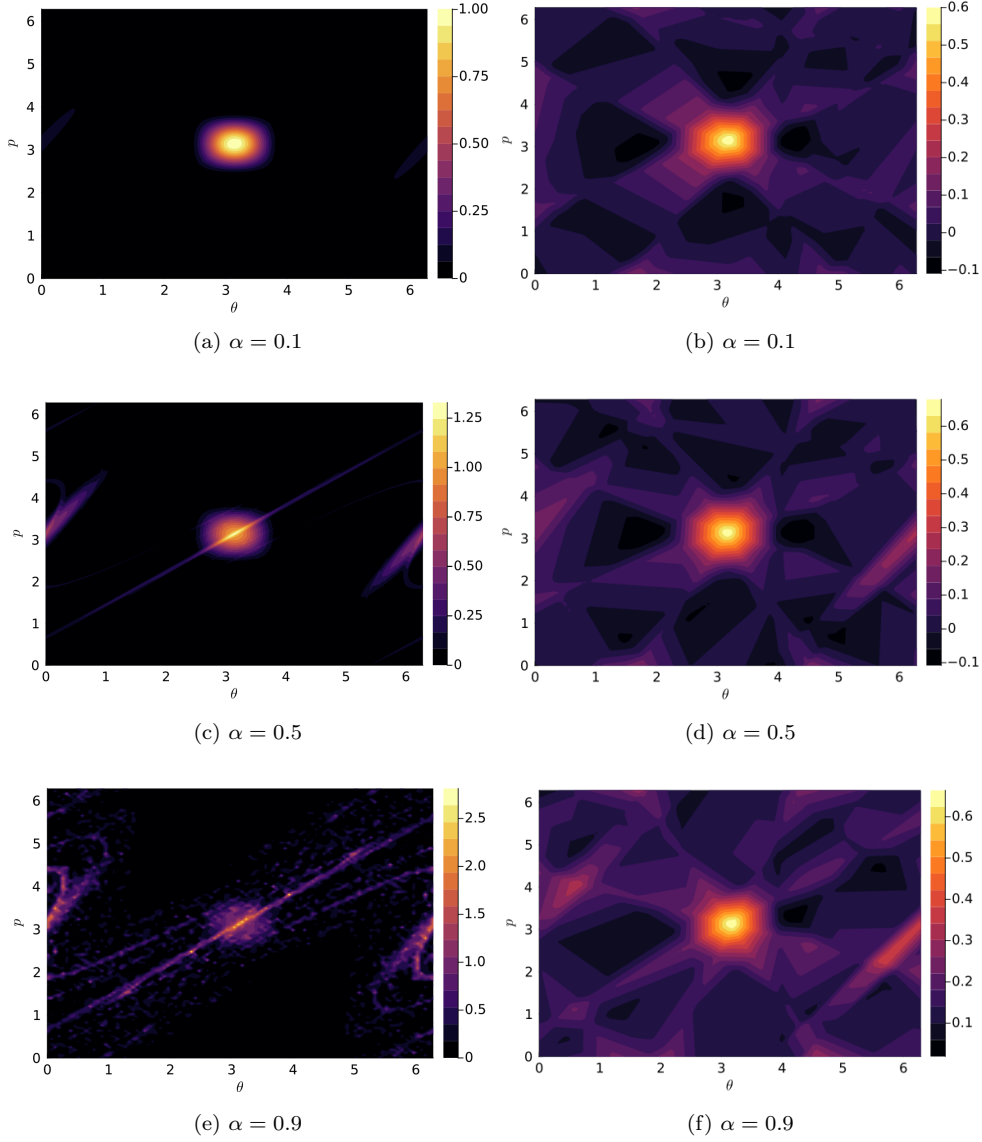


Fig. 8: Solutions computed by the truncated sum with 1,000 terms (left) and PINNs approximation (right) for the standard map example with different values of  $\alpha$ .

we have

$$|l(v)| = \left| \int_{\Omega} f_0 v d\mu \right| \leq \|f_0\|_{L^p} \|v\|_{L^q}.$$

3. Inf-sup stability: For  $u \in L^p(\Omega)$ , by substituting  $v = (u - \alpha \mathcal{P}u)^{p-1} \in L^q(\Omega)$ ,



and using the reverse triangle inequality and assumption (A2), we have

$$\begin{aligned} \sup_{0 \neq v \in L^q(\Omega)} \frac{b(u, v)}{\|v\|_{L^q}} &= \sup_{0 \neq v \in L^q(\Omega)} \frac{\int_{\Omega} (u - \alpha \mathcal{P}u) v d\mu}{\|v\|_{L^q}} \\ &\geq \frac{\int_{\Omega} (u - \alpha \mathcal{P}u)^p d\mu}{\|(u - \alpha \mathcal{P}u)^{p-1}\|_{L^q}} = \frac{\|u - \alpha \mathcal{P}u\|_{L^p}^p}{\|u - \alpha \mathcal{P}u\|_{L^p}^{p/q}} \\ &= \|u - \alpha \mathcal{P}u\|_{L^p} \geq \|u\|_{L^p} - \alpha \|\mathcal{P}u\|_{L^p} \geq (1 - \alpha) \|u\|_{L^p}. \end{aligned}$$

4. Adjoint injectivity: Let  $v \in L^q(\Omega)$  and assume that  $b(u, v) = 0 \quad \forall u \in L^p(\Omega)$ . By choosing  $u = v^{q-1} \in L^p(\Omega)$ , and using Hölder's inequality and the assumption (A2), we have

$$\begin{aligned} 0 &= \int_{\Omega} (v^{q-1} - \alpha \mathcal{P}v^{q-1}) v d\mu = \int_{\Omega} v^q d\mu - \alpha \int_{\Omega} (\mathcal{P}v^{q-1}) v d\mu \\ &\geq \|v\|_{L^q}^q - \alpha \|\mathcal{P}v^{q-1}\|_{L^p} \|v\|_{L^q} \geq \|v\|_{L^q}^q - \alpha \|v^{q-1}\|_{L^p} \|v\|_{L^q} \\ &= \|v\|_{L^q}^q - \alpha \|v\|_{L^q}^{q/p} \|v\|_{L^q} = (1 - \alpha) \|v\|_{L^q}^q. \end{aligned}$$

Hence,  $\|v\|_{L^q} = 0$ , i.e.,  $v = 0$ .  $\square$

#### Appendix B. Equivalent form of RVPINNs loss function.

For  $u_{\theta} \in \mathcal{M}_n \subset L^p(\Omega)$  and  $v_M \in V_M \subset L^q(\Omega)$ , we define

$$r(u_{\theta}, v_M) := l(v_M) - b(u_{\theta}, v_M).$$

Suppose that  $\tilde{g}_{\theta} \in V_M$  is the solution of the following problem:

$$(B.1) \quad \langle J_M(\tilde{g}_{\theta}), v_M \rangle_{L^p, L^q} = r(u_{\theta}, v_M), \quad \text{for all } v_M \in V_M,$$

where  $\langle \cdot, \cdot \rangle_{L^p, L^q}$  denotes the duality pairing and  $J_M$  is the duality map on a subspace  $V_M$  defined by  $J_M(g) = \|g\|_{L^q}^{2-q} |g|^{q-1} \text{sign}(g)$  (see [22]). The following expressions are equivalent:

1.  $\sup_{0 \neq v_M \in V_M} \frac{l(v_M) - b(u_{\theta}, v_M)}{\|v_M\|_{L^q}},$
2.  $\sup_{0 \neq v_M \in V_M} \frac{b(u - u_{\theta}, v_M)}{\|v_M\|_{L^q}},$  where  $u$  is the solution of problem (2.5),
3.  $\|J_M(\tilde{g}_{\theta})\|_{L^p}.$

Indeed, the equivalence of 1. and 2. follows from  $b(u, v_M) = l(v_M) \quad \forall v_M \in V_M$  and the linearity of  $b$ . The equivalence of 1. and 3. follows from

$$\begin{aligned} \sup_{0 \neq v_M \in V_M} \frac{l(v_M) - b(u_{\theta}, v_M)}{\|v_M\|_{L^q}} &= \sup_{0 \neq v_M \in V_M} \frac{r(u_{\theta}, v_M)}{\|v_M\|_{L^q}} \\ &= \sup_{0 \neq v_M \in V_M} \frac{\langle J_M(\tilde{g}_{\theta}), v_M \rangle_{L^p, L^q}}{\|v_M\|_{L^q}} = \|J_M(\tilde{g}_{\theta})\|_{L^p} \end{aligned}$$

where the second equality follows from (B.1) and the third one from the fact that  $v_M = J_M(\tilde{g}_{\theta})$  is the supremizer.

Thus, the RVPINNs loss function can be written in three different forms:

$$1. \quad \mathcal{L}_{\text{RVPINNs}}(u_{\theta}) = \sup_{0 \neq v_M \in V_M} \frac{l(v_M) - b(u_{\theta}, v_M)}{\|v_M\|_{L^q}},$$

2.  $\mathcal{L}_{\text{RVPINNs}}(u_\theta) = \sup_{0 \neq v_M \in V_M} \frac{b(u - u_\theta, v_M)}{\|v_M\|_{L^q}},$
3.  $\mathcal{L}_{\text{RVPINNs}}(u_\theta) = \|J_M(\tilde{g}_\theta)\|_{L^p}.$

Now, consider the case where  $u$  is the solution of the variational problem (2.5) with  $U = V = L^2(\Omega)$ , and  $u_\theta \in \mathcal{M}_n \subset L^2(\Omega)$ . Let  $V_M$  be a finite-dimensional subspace of  $L^2(\Omega)$  with an orthonormal basis  $\{g_1, \dots, g_M\}$ . In this setting, the duality paring in (B.1) corresponds to the  $L^2$ -inner product, and the duality map  $J_M(\tilde{g}_\theta)$  is the Riesz representation in  $V_M$  of  $r(u_\theta, \cdot)$ . Suppose that  $g_\theta \in V_M$  is the solution of the following Galerkin problem:

$$\langle g_\theta, v_M \rangle_{L^2} = r(u_\theta, v_M), \quad \text{for all } v_M \in V_M.$$

Since  $g_\theta \in V_M$ , it can be written as

$$(B.2) \quad g_\theta = \sum_{m=1}^M \alpha_m g_m, \quad \text{where } \alpha_m \in \mathbb{R}, m = 1, 2, \dots, M.$$

For each  $m \in \{1, 2, \dots, M\}$ , we compute the coefficients  $\alpha_m$  by

$$\alpha_m = \langle g_\theta, g_m \rangle_{L^2} = r(u_\theta, g_m).$$

Substituting these into (B.2), we get

$$g_\theta = \sum_{m=1}^M r(u_\theta, g_m) g_m.$$

Taking the  $L^2$ -norm on both sides, we obtain

$$\|g_\theta\|_{L^2} = \sqrt{\sum_{m=1}^M r^2(u_\theta, g_m)}.$$

Thus, the RVPINNs loss function for solutions in  $L^2(\Omega)$  is

$$\mathcal{L}_{\text{RVPINNs}}(u_\theta) = \sqrt{\sum_{m=1}^M \left( \int_{\Omega} (f_0 - u_\theta + \alpha \mathcal{P} u_\theta) g_m d\mu \right)^2}.$$

### Appendix C. Error estimate proofs for PINNs and RVPINNs.

#### Proof of Theorem 4.2.

For arbitrary  $u_\theta \in \mathcal{M}_n$ , by using the assumption (A2), the reverse triangle inequality, the definition of a quasi-minimizer, and the triangle inequality, we have

$$\begin{aligned} (1 - \alpha) \|u - u_{\theta^*}\|_{L^p} &\leq \|u - u_{\theta^*}\|_{L^p} - \alpha \|\mathcal{P}(u - u_{\theta^*})\|_{L^p} \\ &\leq \|(u - u_{\theta^*}) - \alpha \mathcal{P}(u - u_{\theta^*})\|_{L^p} \\ &= \|f_0 - u_{\theta^*} + \alpha \mathcal{P} u_{\theta^*}\|_{L^p} \\ &\leq \|f_0 - u_\theta + \alpha \mathcal{P} u_\theta\|_{L^p} + \delta_n \\ &= \|(u - u_\theta) - \alpha \mathcal{P}(u - u_\theta)\|_{L^p} + \delta_n \\ &\leq \|u - u_{\theta^*}\|_{L^p} + \alpha \|\mathcal{P}(u - u_{\theta^*})\|_{L^p} + \delta_n \\ &\leq (1 + \alpha) \|u - u_\theta\|_{L^p} + \delta_n. \end{aligned}$$

Dividing by  $1 - \alpha$  and taking the infimum over all possible  $u_\theta \in \mathcal{M}_n$  yields the theorem.

In RVPINNs, the local Fortin's condition provides the following result, which is necessary for proving Theorem 4.3.

LEMMA C.1. *Let  $\delta_n > 0$  and  $u_{\theta^*} \in \mathcal{M}_n$  be a quasi-minimizer of (3.4) satisfying (4.1). If the local Fortin's condition is satisfied, it holds:*

$$\|u_{\theta^*} - u_\theta\|_{L^p} \leq \frac{C_\Pi}{1 - \alpha} \left( \sup_{0 \neq v_M \in V_M} \frac{b(u_{\theta^*} - u_\theta, v_M)}{\|v_M\|_{L^q}} \right), \quad \forall u_\theta \in \mathcal{M}_n^{\theta^*, R}.$$

*Proof.* By using the local Fortin's condition and the inf-sup stability in Theorem A.1, we have

$$\begin{aligned} \sup_{0 \neq v_M \in V_M} \frac{b(u_{\theta^*} - u_\theta, v_M)}{\|v_M\|_{L^q}} &\geq \sup_{0 \neq v \in L^q(\Omega)} \frac{b(u_{\theta^*} - u_\theta, \Pi_\theta v)}{\|\Pi_\theta v\|_{L^q}} \\ &= \sup_{0 \neq v \in L^q(\Omega)} \frac{b(u_{\theta^*} - u_\theta, v)}{\|\Pi_\theta v\|_{L^q}} \\ &\geq \frac{1}{C_\Pi} \sup_{0 \neq v \in L^q(\Omega)} \frac{b(u_{\theta^*} - u_\theta, v)}{\|v\|_{L^q}} \\ &\geq \frac{1 - \alpha}{C_\Pi} \|u_{\theta^*} - u_\theta\|_{L^p}. \end{aligned}$$

Multiplying both sides by  $\frac{C_\Pi}{1 - \alpha}$  yields the lemma.  $\square$

#### Proof of Theorem 4.3.

For any  $u_\theta \in \mathcal{M}_n^{\theta^*, R}$ , by using the triangle inequality, Lemma C.1, the definition of a quasi-minimizer, and the boundedness of  $b(\cdot, \cdot)$ , we have

$$\begin{aligned} \|u - u_{\theta^*}\|_{L^p} &\leq \|u_{\theta^*} - u_\theta\|_{L^p} + \|u - u_\theta\|_{L^p} \\ &\leq \frac{C_\Pi}{1 - \alpha} \left( \sup_{0 \neq v_M \in V_M} \frac{b(u_{\theta^*} - u_\theta, v_M)}{\|v_M\|_{L^q}} \right) + \|u - u_\theta\|_{L^p} \\ &\leq \frac{C_\Pi}{1 - \alpha} \left( \sup_{0 \neq v_M \in V_M} \frac{b(u - u_\theta, v_M)}{\|v_M\|_{L^q}} + \sup_{0 \neq v_M \in V_M} \frac{b(u - u_{\theta^*}, v_M)}{\|v_M\|_{L^q}} \right) \\ &\quad + \|u - u_\theta\|_{L^p} \\ &\leq \frac{C_\Pi}{1 - \alpha} \left( 2 \sup_{0 \neq v_M \in V_M} \frac{b(u - u_\theta, v_M)}{\|v_M\|_{L^q}} + \delta_n \right) + \|u - u_\theta\|_{L^p} \\ &\leq \frac{2C_\Pi}{1 - \alpha} (1 + \alpha) \|u - u_\theta\|_{L^p} + \left( \frac{C_\Pi}{1 - \alpha} \right) \delta_n + \|u - u_\theta\|_{L^p} \\ &= \left( 1 + \frac{2C_\Pi}{1 - \alpha} (1 + \alpha) \right) \|u - u_\theta\|_{L^p} + \left( \frac{C_\Pi}{1 - \alpha} \right) \delta_n. \end{aligned}$$

Taking the infimum over all possible  $u_\theta \in \mathcal{M}_n^{\theta^*, R}$  yields the theorem.

#### REFERENCES

- [1] M. AINSWORTH AND J. T. ODEN, *A posteriori error estimation in finite element analysis*, Computer methods in applied mechanics and engineering, 142 (1997), pp. 1–88.
- [2] E. A. ANTONELLO, E. CAMPONOGARA, L. O. SEMAN, J. P. JORDANOU, E. R. DE SOUZA, AND J. F. HÜBNER, *Physics-informed neural nets for control of dynamical systems*, Neurocomputing, 579 (2024), p. 127419.
- [3] S. BERRONE, C. CANUTO, AND M. PINTORE, *Solving PDEs by variational physics-informed neural networks: an a posteriori error analysis*, ANNALI DELL’UNIVERSITA’DI FERRARA, 68 (2022), pp. 575–595.
- [4] S. BERRONE, C. CANUTO, AND M. PINTORE, *Variational physics informed neural networks: the role of quadratures and test functions*, Journal of Scientific Computing, 92 (2022), p. 100.
- [5] C. BOSE AND R. MURRAY, *The exact rate of approximation in Ulam’s method*, Discrete and continuous dynamical systems, 7 (2000), pp. 219–235.
- [6] I. BREVIS, I. MUGA, AND K. G. VAN DER ZEE, *Neural control of discrete weak formulations: Galerkin, least squares & minimal-residual methods with quasi-optimal weights*, Computer Methods in Applied Mechanics and Engineering, 402 (2022), p. 115716.
- [7] S. CAI, Z. MAO, Z. WANG, M. YIN, AND G. E. KARNIAKAKIS, *Physics-informed neural networks (PINNs) for fluid mechanics: A review*, Acta Mechanica Sinica, 37 (2021), pp. 1727–1738.
- [8] Z. CAI, J. CHEN, M. LIU, AND X. LIU, *Deep least-squares methods: An unsupervised learning-based numerical method for solving elliptic PDEs*, Journal of Computational Physics, 420 (2020), p. 109707.
- [9] S. CUOMO, V. S. DI COLA, F. GIAMPAOLO, G. ROZZA, M. RAISSI, AND F. PICCIALLI, *Scientific machine learning through physics-informed neural networks: Where we are and what’s next*, Journal of Scientific Computing, 92 (2022), p. 88.
- [10] R. R. FARIA, B. CAPRON, A. R. SECCHI, AND M. B. DE SOUZA JR, *A data-driven tracking control framework using physics-informed neural networks and deep reinforcement learning for dynamical systems*, Engineering Applications of Artificial Intelligence, 127 (2024), p. 107256.
- [11] G. FROYLAND, R. M. STUART, AND E. VAN SEBILLE, *How well-connected is the surface of the global ocean?*, Chaos: An Interdisciplinary Journal of Nonlinear Science, 24 (2014).
- [12] I. GÜHRING, M. RASLAN, AND G. KUTYNIK, *Expressivity of Deep Neural Networks*, Cambridge University Press, 2022, p. 149–199.
- [13] T. HARTMANN, S. MORITA, G. TANNER, AND D. J. CHAPPELL, *High-frequency structure-and air-borne sound transmission for a tractor model using dynamical energy analysis*, Wave Motion, 87 (2019), pp. 132–150.
- [14] E. KAISER, J. N. KUTZ, AND S. L. BRUNTON, *Data-driven approximations of dynamical systems operators for control*, The Koopman operator in systems and control: concepts, methodologies, and applications, (2020), pp. 197–234.
- [15] E. KHARAZMI, Z. ZHANG, AND G. E. KARNIAKAKIS, *Variational physics-informed neural networks for solving partial differential equations*, arXiv preprint arXiv:1912.00873, (2019).
- [16] E. KHARAZMI, Z. ZHANG, AND G. E. KARNIAKAKIS, *hp-VPINNs: Variational physics-informed neural networks with domain decomposition*, Computer Methods in Applied Mechanics and Engineering, 374 (2021), p. 113547.
- [17] S. KLUS, P. KOLTAI, AND C. SCHÜTTE, *On the numerical approximation of the Perron-Frobenius and Koopman operator*, arXiv preprint arXiv:1512.05997, (2015).
- [18] A. LASOTA AND M. C. MACKEY, *Chaos, fractals, and noise: stochastic aspects of dynamics*, vol. 97, Springer Science & Business Media, 2013.
- [19] K. LINKA, A. SCHÄFER, X. MENG, Z. ZOU, G. E. KARNIAKAKIS, AND E. KUHL, *Bayesian physics informed neural networks for real-world nonlinear dynamical systems*, Computer Methods in Applied Mechanics and Engineering, 402 (2022), p. 115346.
- [20] B. LUSCH, J. N. KUTZ, AND S. L. BRUNTON, *Deep learning for universal linear embeddings of nonlinear dynamics*, Nature communications, 9 (2018), p. 4950.
- [21] I. MUGA, M. J. TYLER, AND K. G. VAN DER ZEE, *The discrete-dual minimal-residual method (ddmres) for weak advection-reaction problems in banach spaces*, Computational Methods in Applied Mathematics, 19 (2019), pp. 557–579.
- [22] I. MUGA AND K. G. VAN DER ZEE, *Discretization of linear problems in Banach spaces: Residual minimization, nonlinear Petrov–Galerkin, and monotone mixed methods*, SIAM Journal on Numerical Analysis, 58 (2020), pp. 3406–3426.
- [23] E. O. OLUWASAKIN AND A. Q. KHALIQ, *Optimizing physics-informed neural network in dynamic system simulation and learning of parameters*, Algorithms, 16 (2023), p. 547.
- [24] D. ONKEN, L. NURBEKYAN, X. LI, S. W. FUNG, S. OSHER, AND L. RUTHOTTO, *A neural network approach for high-dimensional optimal control applied to multiagent path finding*, IEEE Transactions on Control Systems Technology, 31 (2022), pp. 235–251.

- [25] P. PETERSEN, M. RASLAN, AND F. VOIGTLAENDER, *Topological properties of the set of functions generated by neural networks of fixed size*, Foundations of computational mathematics, 21 (2021), pp. 375–444.
- [26] M. RAISSI, P. PERDIKARIS, AND G. E. KARNIADAKIS, *Physics-informed neural networks: A deep learning framework for solving forward and inverse problems involving nonlinear partial differential equations*, Journal of Computational physics, 378 (2019), pp. 686–707.
- [27] M. RICHTER, D. J. CHAPPELL, AND G. TANNER, *Convergence of ray-based methods using transfer operators in different bases*, in Forum acousticum, 2020.
- [28] S. ROJAS, P. MACZUGA, J. MUÑOZ-MATUTE, D. PARDO, AND M. PASZYŃSKI, *Robust variational physics-informed neural networks*, Computer Methods in Applied Mechanics and Engineering, 425 (2024), p. 116904.
- [29] S. SAQLAIN, W. ZHU, E. G. CHARALAMPIDIS, AND P. G. KEVREKIDIS, *Discovering governing equations in discrete systems using PINNs*, Communications in Nonlinear Science and Numerical Simulation, 126 (2023), p. 107498.
- [30] J. SIRIGNANO AND K. SPILIOPOULOS, *Dgm: A deep learning algorithm for solving partial differential equations*, Journal of computational physics, 375 (2018), pp. 1339–1364.
- [31] J. SLIPANTSCHUK, M. RICHTER, D. J. CHAPPELL, G. TANNER, W. JUST, AND O. F. BANDTLOW, *Transfer operator approach to ray-tracing in circular domains*, Nonlinearity, 33 (2020), p. 5773.
- [32] A. TANTET, V. LUCARINI, F. LUNKEIT, AND H. A. DIJKSTRA, *Crisis of the chaotic attractor of a climate model: a transfer operator approach*, Nonlinearity, 31 (2018), p. 2221.
- [33] A. TANTET, F. R. VAN DER BURGT, AND H. A. DIJKSTRA, *An early warning indicator for atmospheric blocking events using transfer operators*, Chaos: An Interdisciplinary Journal of Nonlinear Science, 25 (2015).
- [34] S. M. ULAM, *A Collection of Mathematical problems*, Interscience Tracts in Pure and Applied Mathematics, 1960.
- [35] U. VAIDYA, P. G. MEHTA, AND U. V. SHANBHAG, *Nonlinear stabilization via control lyapunov measure*, IEEE Transactions on Automatic Control, 55 (2010), pp. 1314–1328.
- [36] B. YU ET AL., *The deep ritz method: a deep learning-based numerical algorithm for solving variational problems*, Communications in Mathematics and Statistics, 6 (2018), pp. 1–12.
- [37] R. YU AND R. WANG, *Learning dynamical systems from data: An introduction to physics-guided deep learning*, Proceedings of the National Academy of Sciences, 121 (2024), p. e2311808121.